Bioorganic & Medicinal Chemistry Letters 21 (2011) 6042–6048

Contents lists available at SciVerse ScienceDirect

Bioorganic & Medicinal Chemistry Letters

journal homepage: www.elsevier.com/locate/bmcl

Design, synthesis and SAR of indazole and benzoisoxazole containing 4-azetidinyl-1-aryl-cyclohexanes as CCR2 antagonists

Xuqing Zhang*, Heather Hufnagel, Cuifen Hou, Evan Opas, Sandra McKenney, Carl Crysler, John O'Neill, Dana Johnson, Zhihua Sui

Johnson & Johnson Pharmaceutical Research and Development, Welsh & McKean Roads, Spring House, PA 19477, United States

ARTICLE INFO

Article history:
Received 19 June 2011
Revised 11 August 2011
Accepted 15 August 2011
Available online 22 August 2011

Keywords:
CCR2
Indazole
Benzoisoxazole

ABSTRACT

A novel series of 4-azetidinyl-1-aryl-cyclohexanes containing indazole or benzoisoxazole moiety have been identified as potent CCR2 antagonists with high selectivity versus hERG.

MCP-1 is a potent chemotactic factor for monocytes and memory T lymphocytes, and stimulates the movement of those cells along a chemotactic gradient following binding to its cell-surface receptor, CC chemokine receptor-2 (CCR2). MCP-1 interacts exclusively with CCR2 and is therefore recognized as the prime CCR2 ligand.[1–5] This ligand/receptor pair is overexpressed in numerous inflammatory conditions wherein excessive monocyte recruitment is observed. Indeed, CCR2- and MCP-1-deficient mice and CCR2 or MCP-1 antibody-treated rodents show decreased recruitment of monocytes and produce markedly attenuated inflammatory responses in animal models of multiple sclerosis, rheumatoid arthritis, atherosclerosis, diabetes, asthma, allograft rejection, and neuropathic pain.[6–15] Clearly, these observations confirm the role of CCR2 in the pathogenesis of several immune-based inflammatory diseases and identify this chemokine receptor as a potentially valuable therapeutic target. An antagonist of the binding of MCP-1 to its receptor CCR2 may be an effective treatment for any inflammatory disease in which monocytes, mast cells, or basophils play major roles. As a result, there has been significant interest in the design and synthesis of CCR2 antagonists.[16–34]

We have recently described azetidinyl cyclohexane scaffold bearing two consecutive amide bonds as potent CCR2 antagonists with good selectivity versus hERG.[35] However, this type of functionality is prone to rapid metabolism in vivo, which might lead to low exposure. We describe herein our exploration on amide replacements.[36,37] We were guided by the result from compound **1** in our early series (Fig. 1). Installation of *ortho*-amino group at the right side of the phenyl ring was well tolerated for CCR2 binding affinity and functional activities. Encouraged by this finding, we investigated fusion strategy between amino group and its neighboring amide group. Hence, compounds **2**–**5** bearing 5/6-fused ring systems have been synthesized and their CCR2 binding affinity is summarized in Table 1. Direct connection of the *ortho*-amino and the amide nitrogen dramatically reduced CCR2 binding affinity as shown in **2** with IC_{50} of 5.4 μM. To our delight, moving the amide to the 3-position of the five-membered heterocycle to form an aromatic system provided compounds reasonable CCR2 binding affinity (compounds **3–5**). Compound **5** bearing amino indazole moiety was particularly interesting because it improved CCR2 binding affinity by threefold compared to its diamide counterpart (**1**, IC_{50} 46 nM).[35] Detailed SAR and

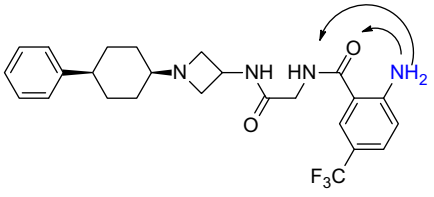

1
hCCR2 binding, IC_{50}, 46 nM
hCCR2 function (CTX), IC_{50}, 9 nM

Figure 1. Design of 5,6-fused ring system.

* Corresponding author.
E-mail address: xzhang5@prdus.jnj.com (X. Zhang).

0960-894X/$ - see front matter © 2011 Elsevier Ltd. All rights reserved.
doi:10.1016/j.bmcl.2011.08.074

Table 1

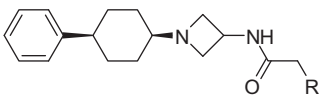

A

ID	R	CCR2 binding[a] IC_{50} (nM)
2	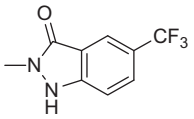	5,400[c]
3	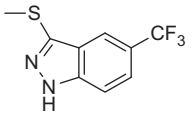	290[c]
4	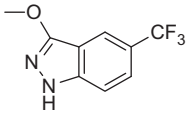	510[c]
5	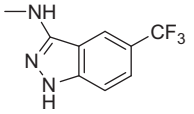	12[b]

[a] MCP-1 receptor binding assay in THP-1 cells, see Ref. 38.
[b] IC_{50} value is reported as the average of two separate determinations with variation of ±15%.
[c] IC_{50} values are reported from single determination.

optimization of this novel series containing 5/6-fused ring system were warranted. Since this scaffold is derived from the diamide series, we faced similar challenges in hERG liability. Hence, our goal is to identify lead compounds with potent CCR2 activity and high selectivity with respect to hERG activity.

The synthesis of the target compounds in this series is shown in Scheme 1. 2-Fluoro-benzonitrile **6** was condensed with commercially available hydrazine (R^2NHNH_2) in refluxing IPA to afford the corresponding indazoles **7** (77–95% yield). A second route to indazoles **7** was developed to synthesize analogs inaccessible from direct coupling of **6** and substituted hydrazines. Thus, **6** was reacted with NH_2NH_2 to form un-substituted indazole intermediate (92% yield), which was then protected as phthalimide **6a** by treating with phthalic anhydride (70% yield), followed by sulfonylation (for compound **14t**, MsCl, TEA, 81% yield), acyclation (for compounds **13h**, **13i**, **14s**, **16l**, *t*-Bu-NCO, 85% yield) or alkylation (for compounds **14q**, **14r**, **14u**, and **14v**, NaH, R^2Br, 65–75% yield). After de-protection of phthalimide (50–72% yield), the corresponding indazoles **7** were obtained. For the benzoisoxazole analogs, compound **6** was reacted with acetohydroxamic acid by treatment with *t*-BuOK to afford intermediate **8** (71% yield). The resulting 5/6-fused amino indazoles **7** or benzoisoxazoles **8** were converted to acids **9** by reductive amination with glyoxylic acid using $NaBCNH_3$ (75–80% yield). Azetidine intermediates **11** were obtained by coupling of **9** and amino azetidine **10** under EDCI (65–88% yield). Target compounds were obtained by reductive amination with $NaBH(OAc)_3$ of azetidines **11** and ketones **12** in 55–85% overall yield. The cis isomer (**13**–**16**) and trans isomers (**17**) were separated in 2.5:1 to 1:1 ratio and evaluated individually in the biological assays. Ketones **12** were synthesized according to our early Letter.[35]

We began our SAR exploration on the left side R^1 group of indazoles **B** shown in Table 2. Consistent with the SAR of the diamide series, modification on the left side aromatic or hetero-aromatic R^1 group was well tolerated for CCR2 binding affinity,[38] as evidenced by compounds bearing electron neutral (**13a**), electron rich (**13b** and **13e**), polar phenyl ring (**13c**), or heterocyclic ring (**13d**). Unfortunately, these compounds exhibited strong hERG binding affinity which could be related to the chemo-type containing a central basic amine flanked by two aromatic rings. While displaying weaker CCR2 binding and functional activity,[39] compound **13f** was quite interesting since it also presented weaker hERG binding affinity (IC_{50} of 34 μM).[40] Structurally, compound **13f** contained a partially unsaturated pyridone substitution at the R^1 position, which indicated that nonaromatic R^1 might be tolerated for CCR2 activity and may increase selectivity versus hERG. To explore this hypothesis, we synthesized a sub-set of derivatives (**14a**–**14n**) bearing nonaromatic R^1 group and evaluated both CCR2 and hERG affinity. In contrast to their diamide analogs which were usually inactive in CCR2 (binding IC_{50} >25 μM, data not shown), nonaromatic R^1 substituted indazoles **14** displayed moderate to good CCR2 binding and functional activity. As illustrated by **14a** and **14b**, installation of *i*-Pr or CN group at the R^1 position exhibited CCR2 binding affinity to sub-μM. Incorporation of more lipophilic cyclohexanyl group (**14c**) slightly increased CCR2 binding affinity as compared to **14a**. To our delight, ethyl carboxylate substituted indazole **14d** displayed comparable CCR2 antagonistic activity as its aromatic substituted analogs (binding IC_{50} of 13 nM, CTX IC_{50} of 40 nM). Unfortunately, **14d** showed no improvement on attenuating hERG affinity. While significantly decreasing hERG affinity, substitution at the R^1 group with polar groups such as carboxylic acid (**14e**), carbamide (**14f**) or hydroxyl (**14j**) failed to maintain good CCR2 binding affinity. Alcohol **14g** was promising, as it displayed potent CCR2 binding affinity (IC_{50} of 44 nM) with promising (~80-fold) selectivity over hERG. To circumvent the phase II metabolism liability of **14g** due to the primary hydroxyl group, ethyl (**14h**) and allyl ethers (**14i**) were evaluated. These modifications maintained good CCR2 binding affinity but increased hERG inhibition as compared to **14g**. Similar operation by masking alcohol **14j** with ethyl (**14k**) or allyl group (**14l**) only yielded moderate enhancement on CCR2 binding affinity. Substitution containing amino group either dramatically reduced or completely abolished CCR2 binding affinity as shown by **14m** and **14n**.

Next we conducted SAR studies at the R^2 substitution on indazole ring. 3,4-Methlenedioxy-phenyl and ethyl carboxylate groups were selected as two representative R^1 substitutions for R^2 SAR studies. As illustrated in Table 3, benzoisoxazoles **15a** and **15b** offered no improvement on dialing out hERG compared to their corresponding indazoles **13b** and **14o**. Substitution on 1-position of the indazole ring indicated there is room for modifications. Small lipophilic alkyl groups (**14d**, **14p**, and **14q**) as well as hydroxyethyl group (**13g**) were well tolerated for CCR2 activity. Surprisingly, trifluoroethyl substituted indazole **14r** displayed more than 10-fold potency drop compared with its hydrocarbon analog **14p**. In an attempt to improve CCR2/hERG selectivity, polar substitutions were introduced onto the indazole ring. Urea substituted indazole **13i** and **14s** displayed good CCR2 activity and trend to decrease hERG binding affinity (IC_{50} of 12 and 20 μM). Methyl sulfonylation of indazole ring substantially reduced CCR2 binding affinity as shown in **14t** (IC_{50} of 920 nM). Steric bulky substitutions such as benzyl or cyclopentyl ring also decreased CCR2 activity (**14u** and **14v**). It was apparent that polar substitutions especially with H-bonding donors could significantly suppress hERG affinity. However, compounds containing this feature possess potential poor physical characteristics such as low aqueous solubility, poor intestinal permeability (uera), and conjugate formation (primary alcohol).[41]

Inspired by our early findings on azetidinyl diamide series that incorporation of 1-hydroxy group at the cyclohexanyl ring efficiently suppressed hERG affinity, we prepared a sub-set of compounds bearing 1-hydroxy substitution on the cyclohexanyl ring

(Table 4). While in diamide series the hydroxy analogs generally displayed weaker CCR2 activity as compared to the corresponding des-oxy derivatives, introduction of 1-hydroxyl group into 5,6-fused indazoles and benzoisoxazoles was well tolerated for good CCR2 activity. For examples, indazoles **16a** and **16b** exhibited slight gain in CCR2 binding affinity over their corresponding diamide analogs (IC_{50} of 19 and 5 nM vs 36 and 15 nM).[35] For electron deficient R^1 group such as pyridinyl substitution, hydroxyl indazole **16c** gained sixfold in affinity for CCR2 as compared to its diamide analog (IC_{50} of 190 nM) without increasing hERG affinity (IC_{50} of 36 μM).[35] Encouraged by this finding, we then turned our effort to refine SAR of various heterocyclic substitutions at the R^1 position. Installation of electron donating group such as methoxy (**16g**) or methyl (**16h**) on pyridinyl ring exhibited an increase in CCR2 affinity as compared to its un-substituted analog **16f**. Both 2-thiazoyl (**16i**) and 5-thiazoyl (**16j**) substituted indazoles displayed good CCR2 binding affinity with satisfactory selectivity versus hERG as indicated by hERG binding and patch express studies.[42] As expected, methyl (**16k**), hydroxyethyl (**16m**), or urea (**16l**) substitution on the indazole was tolerated for CCR2 affinity. Substitutions of thiazole ring with lipophilic alkyl groups gave compounds **16n**, **16o**, and **16p** that were equipotent to the unsubstituted thiazole analog **16j** versus CCR2. Unfortunately again, these compounds exhibited an increase in hERG potency compared to **16j** as indicated by both hERG binding affinity and hERG patch express test. Substitutions at the R^1 position with more polar five-membered heterocycles such as oxazole (**16q**), imidazole (**16r**), or pyrazole (**16s**) significantly reduced CCR2 binding affinity. Introduction of a nonaromatic acetylene substitution (**16t**) abolished CCR2 affinity as shown in **16t**. As for benzoisoxazoles **15c**, **15d**, and **15e**, they maintained good CCR2 activity as compared to their indazole analogs. Once again, stronger hERG binding affinity and hERG functional signals in patch express study were observed. Overall, through the SAR study, 5-thiazole as the R^1 substitution in hydroxyl indazoles afforded the resulting compounds with high selectivity over the hERG ion channel.

Thiazole **16j** had overall the best profile and was selected for pharmacokinetic studies.[43] As shown in Table 5, compound **16j** has high clearance and low bioavailability in rats but low clearance (CL, 9.80 mL/min/kg) and good oral bioavailability (F, 75.7%) in dogs.

In summary, we have demonstrated that 5/6-fused rings such as indazole and benzoisoxazole are viable diamide replacements in 4-azetidinyl-1-aryl-cyclohexanes as CCR2 antagonists. Optimization of indazole series according to divergent SARs on both CCR2 and hERG produced compound **16j** with potent CCR2 activity and good selectivity over hERG. Furthermore, the PK profile of **16j**

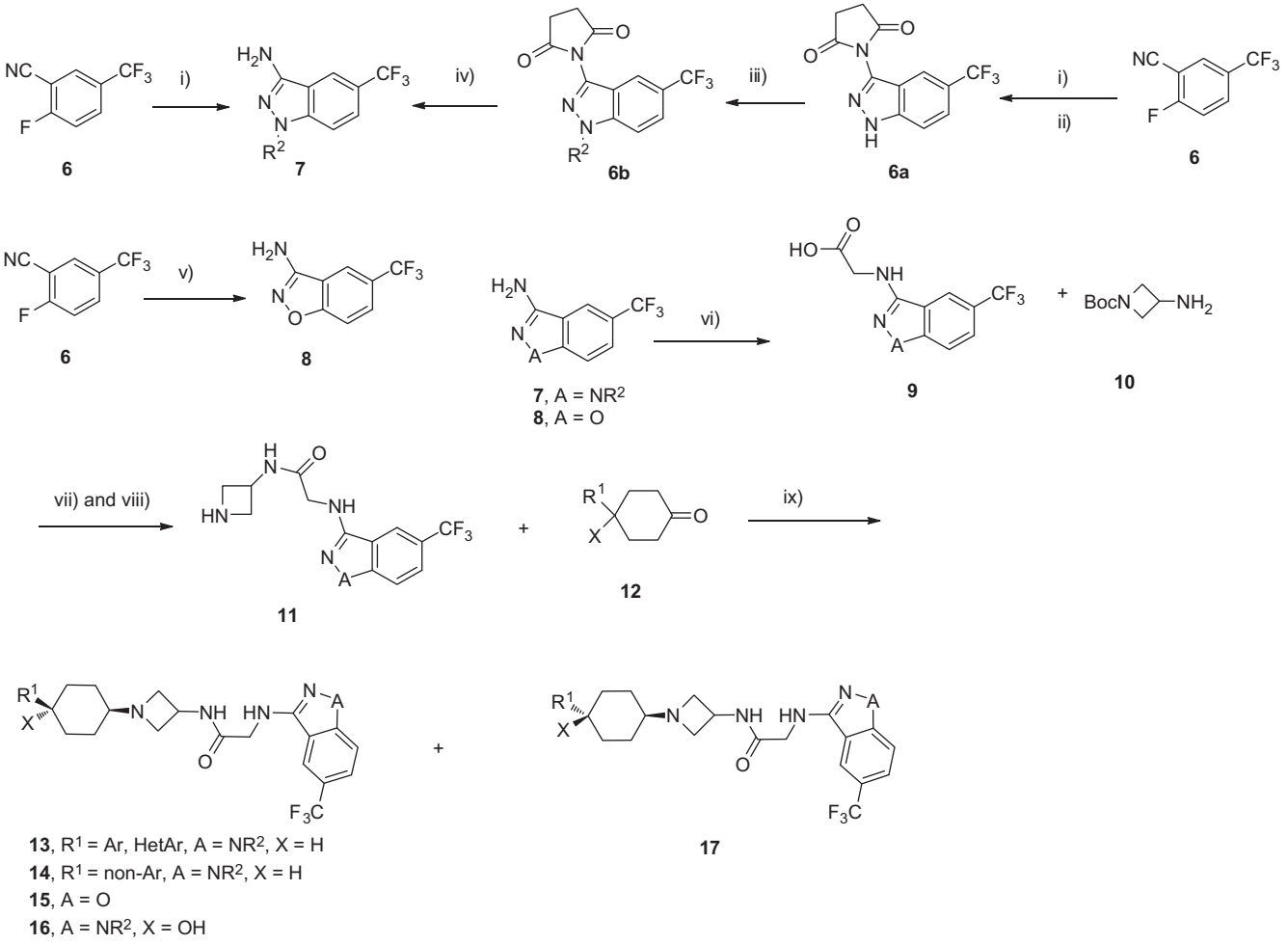

Scheme 1. Reagents and conditions: (i) NH_2NHR^2, IPA, reflux (77–95%); (ii) phthalic anhydride (70%); (iii) for **14t**, MsCl, TEA(81%); for **13h**, **13i**, **14s**, **16l**, *t*-BuNCO, and then TFA (~85%); for **14q**, **14r**, **14u**, **14v**, NaH, $BrCH_2CH{=}CH_2$ or ICH_2CF_3 or BnBr or cyclopentyl-OTs (65–75%); (iv) NH_2NH_2 (50–72%); (v) MeCONHOH, *t*-BuOK (71%); (vi) glyoxylic acid monohydrate, $NaBCNH_3$, MeOH (75–80%); (vii) EDCI, HOBt, TEA; (vii) TFA (65–88%); (ix) $NaBH(OAc)_3$, AcOH, silica gel column separation 5% 7 N NH_3/MeOH in DCM (55–85%).

Table 2

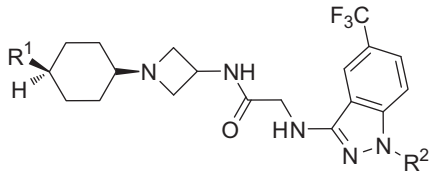

B

ID	R^1	R^2	CCR2 binding[a] IC_{50} (nM)	CTX[a,b] IC_{50} (nM)	hERG binding[c] IC_{50} (μM)
13a		H	12	9	1.20
13b	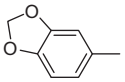	H	6	3	1.1
13c	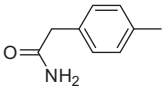	H	12	35	9.5
13d	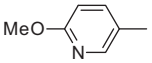	H	12	2	2.5
13e	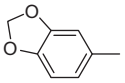	Me	13	8	0.84
13f		H	63	170	34
14a	*i*-Pr	H	370	nt[d]	6.2
14b	CN	Me	330	nt	24
14c		Me	120	nt	3.1
14d	CO_2Et	Me	13	40	8.0
14e	COOH	Me	2,600	nt	25
14f	$CONH_2$	Me	510	nt	32
14g	CH_2OH	Me	44	47	32
14h	CH_2OEt	Me	27	86	5.6
14i	$CH_2OCH_2CH{=}CH_2$	Me	32	66	5.0
14j	OH	Me	530	nt	30
14k	OEt	Me	140	nt	4.5
14l	$OCH_2CH{=}CH_2$	Me	200	nt	7.4
14m	NH_2	Me	>25,000	nt	>50
14n	$NHSO_2Me$	Me	2080	nt	23

[a] IC_{50} values are reported as the average of at least two separate determinations if IC_{50} <100 nM with a typical variation of less than ±25%, for IC_{50} >100 nM, only one test was conducted for IC_{50} determination.
[b] MCP-1 induced chemotaxis in THP-1 cells (Ref. 39).
[c] hERG 3*H*-astemizole binding activity on HEK-293 cell (Ref. 40).
[d] nt, not tested

Table 3

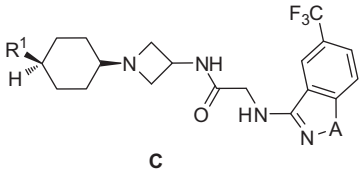

C

ID	R^1	A	CCR2 binding[a] IC_{50} (nM)	CTX IC_{50}[a] (nM)	hERG binding IC_{50} (μM)
13b	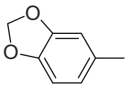	NH	6	3	1.1
15a	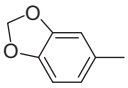	O	36	20	1.9
13g	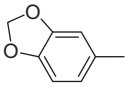	NCH_2CH_2OH	21	20	7.6
13h	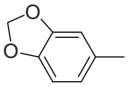	NCONH-t-Bu	55	19	4.7
13i	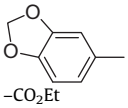	$NCONH_2$	82	34	12
14o	$-CO_2Et$	NH	27	15	9.1
15b	$-CO_2Et$	O	29	34	5.6
14d	$-CO_2Et$	NMe	13	40	8.0
14p	$-CO_2Et$	NEt	15	7	7.6
14q	$-CO_2Et$	$NCH_2CH{=}CH_2$	53	28	3.7
14r	$-CO_2Et$	NCH_2CF_3	230	nt	2.5
14s	$-CO_2Et$	$NCONH_2$	56	14	20
14t	$-CO_2Et$	NSO_2Me	920	nt	25
14u	$-CO_2Et$	Bn	170	67	1.4
14v	$-CO_2Et$		650	nt	4.1

[a] IC_{50} values are reported as the average of at least two separate determinations if IC_{50} <100 nM with a typical variation of less than ±25%, for IC_{50} >100 nM, only one test was conducted for IC_{50} determination.

Table 4

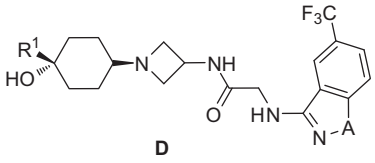

D

ID	R^1	A	CCR2 binding IC_{50} (nM)[a]	CTX IC_{50} (nM)[a]	hERG binding IC_{50} (μM)	hERG patch[b] % @ 3 μM (sov. con.)
16a	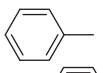	NMe	19	30	10	76 (17)
16b	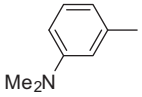	NMe	5	4	12	61 (11)

(*continued on next page*)

Table 4 (*continued*)

ID	R^1	A	CCR2 binding IC_{50} (nM)[a]	CTX IC_{50} (nM)[a]	hERG binding IC_{50} (μM)	hERG patch[b] % @ 3 μM (sov. con.)
16c		NH	30	31	36	31 (15)
16d	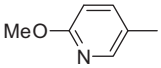	NH	16	10	32	30 (15)
16e	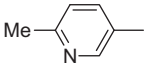	NH	6	11	27	23 (15)
16f		NMe	56	11	24	52 (16)
16g	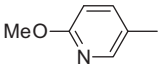	NMe	9	15	12	68 (16)
16h	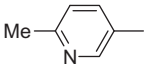	NMe	7	7	18	56 (11)
16i		NH	16	11	>50	17 (17)
16j		NMe	28	14	44	27 (19)
16k		NMe	13	17	27	44 (17)
16l		$NCONH_2$	29	7	31	38 (17)
16m		CH_2CH_2OH	29	22	>50	21 (19)
16n	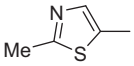	NMe	19	33	25	48 (17)
16o	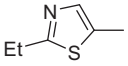	NMe	18	7	23	62 (19)
16p	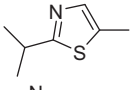	NMe	5	12	17	55 (11)
16q		NMe	480	nt	nt	nt
16r		NMe	1,400	nt	nt	nt
16s	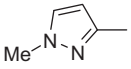	NMe	200	140	>50	nt
16t		NMe	10,000	nt	>50	nt
15c	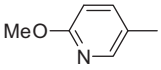	O	23	20	8.7	72 (11)
15d		O	31	37	16	55 (11)
15e		O	31	27	11	72 (18)

[a] IC_{50} values are reported as the average of at least two separate determinations if IC_{50} <100 nM with a typical variation of less than ±25%, for IC_{50} >100 nM, only one test was conducted for IC_{50} determination.

[b] The membrane K^+ current IKr in HERG-transfected HEK293 cells (solvent control), see Ref. 42.

Table 5
Rat and dog PK data for compound **16j**

Species	PO[a] (mpk)	$t_{1/2}$ (h)	C_{max} (ng/μL)	AUC_{last} (h∗ng/μL)	IV[b] (mpk)	V_{ss} (L/kg)	CL (mL/min/kg)	F (%)
Rat	10	—	37±14	56±29	2	7.61±2.62	56.0±16.4	2.35±0.4
Dog	10	5.2±2.1	2973±320	12913±2450	2	1.81±0.45	9.80±3.25	75.7±12.3

[a] PO (10 mg/kg) in 0.5% Methocel (n = 4)
[b] V (2 mg/kg) in 20% HPBCD (n = 4)

proved to be amenable with moderate clearance and volume distribution and high oral bioavailability in dogs. The lead compound from this series therefore deserves to be further explored in in vivo efficacy models to exploit the therapeutic potential for inflammation and metabolic diseases.

Acknowledgments

We thank Lead Generation Biology, Center of Excellence for Cardiovascular Safety Research and ADME/PK teams at J&J PRD for their technical assistance.

Supplementary data

Supplementary data associated with this article can be found, in the online version, at doi:10.1016/j.bmcl.2011.08.074.

References and notes

1. Charo, I. F.; Ransohoff, R. M. *N. Engl. J. Med.* **2006**, *354*, 610.
2. Campbell, E. M.; Charo, I. F.; Kunkel, S. L.; Strieter, R. M.; Boring, L.; Gosling, J.; Lukacs, W. *J. Immunol.* **1999**, *163*, 2160.
3. Okuma, T.; Terasaki, Y.; Kaikita, K.; Kobayashi, H.; Kuziel, W. A.; Kawasuji, M.; Takeya, M. *J. Pathol.* **2004**, *204*, 594.
4. Navratilova, Z. *Biomed. Pap.* **2006**, *150*, 191.
5. Castellani, M. L.; Bhattacharya, K.; Tagen, M.; Kempuraj, D.; Perrella, A.; Delutis, M.; Boucher, W.; Conti, P.; Theoharides, T. C.; Cerulli, G.; Salini, V.; Neri, G. *Int. J. Immunopathol. Pharmacol.* **2007**, *20*, 447.
6. Gong, J. H.; Ratkay, L. G.; Waterfield, J. D.; ClarkLewis, I. *J. Exp. Med.* **1997**, *186*, 131.
7. Ogata, H.; Takeya, M.; Yoshimura, T.; Takagi, K.; Takahashi, K. *J. Pathol.* **1997**, *182*, 106.
8. Huang, D. R.; Wang, J. T.; Kivisakk, P.; Rollins, B. J.; Ransohoff, R. M. *J. Exp. Med.* **2001**, *193*, 713.
9. Izikson, L.; Klein, R. S.; Charo, I. F.; Weiner, H. L.; Luster, A. D. *J. Exp. Med.* **2000**, *192*, 1075.
10. Fife, B. T.; Huffnagle, G. B.; Kuziel, W. A.; Karpus, W. J. *J. Exp. Med.* **2000**, *192*, 899.
11. Dawson, T. C.; Kuziel, W. A.; Osahar, T. A.; Maeda, N. *Atherosclerosis* **1999**, *143*, 205.
12. Kanda, H.; Tateya, S.; Tamori, Y.; Kotani, K.; Hiasa, K. I.; Kitazawa, R.; Kitazawa, S.; Miyachi, H.; Maeda, S.; Egashira, K.; Kasuga, M. *J. Clin. Investig.* **2006**, *116*, 1494.
13. Weisberg, S. P.; Hunter, D.; Huber, R.; Lemieux, J.; Slaymaker, S.; Vaddi, K.; Charo, I.; Leibel, R.; Ferrante, A. W. *J. Clin. Investig.* **2006**, *116*, 115.
14. Kamei, N.; Tobe, K.; Suzuki, R.; Ohsugi, M.; Watanabe, T.; Kubota, N.; Ohtsuka-Kowatari, N.; Kumagai, K.; Sakamoto, K.; Kobayashi, M.; Kadowaki, T. *J. Biol. Chem.* **2006**, *281*, 26602.
15. White, F. A.; Feldman, P.; Miller, R. J. *Mol. Interv.* **2009**, *9*, 188.
16. Struthers, M.; Pasternak, A. *Curr. Top. Med. Chem.* **2010**, *10*, 1278.
17. Xia, M.; Sui, Z. *Expert Opin. Ther. Pat.* **2009**, *19*, 295.
18. Kalinowska, A.; Losy, J. *Expert Opin. Invest. Drug* **2008**, *17*, 1267.
19. Carter, P. H.; Cherney, R. J.; Mangion, I. K. *Annu. Rep. Med. Chem.* **2007**, *42*, 211.
20. Sobhia, M. E.; Singh, R.; Kare, P.; Chavan, S. *Expert Opin. Drug Discovery* **2010**, *5*, 543.
21. Van Lommen, G.; Doyon, J.; Coesemans, E.; Boeckx, S.; Cools, M.; Buntinx, M.; Hermans, B.; VanWauwe, J. *Bioorg. Med. Chem. Lett.* **2005**, *15*, 497.
22. Yang, L.; Zhou, C.; Guo, L.; Morriello, G. J.; Butora, G.; Pasternak, A.; Parsons, W. H.; Mills, S. G.; MacCoss, M.; Vicario, P. P.; Zweerink, H.; Ayala, J. M.; Goyal, S.; Hanlon, W. A.; Cascieri, M. A.; Springer, M. S. *Bioorg. Med. Chem. Lett.* **2006**, *16*, 3735.
23. Butora, G.; Morriello, G. J.; Kothandaraman, S.; Guiadeen, D.; Pasternak, A.; Parsons, W. H.; MacCoss, M.; Vicario, P. P.; Cascieri, M. A.; Yang, L. *Bioorg. Med. Chem. Lett.* **2006**, *16*, 4715.
24. Pasternak, A.; Marino, D.; Vicario, P. P.; Ayala, J. M.; Cascierri, M. A.; Parsons, W.; Mills, S. G.; MacCoss, M.; Yang, L. *J. Med. Chem.* **2006**, *49*, 4801.
25. Zhou, C.; Guo, L.; Parsons, W. H.; Mills, S. G.; MacCoss, M.; Vicario, P. P.; Zweerink, H.; Cascieri, M. A.; Springer, M. S.; Yang, L. *Bioorg. Med. Chem. Lett.* **2007**, *17*, 309.
26. Pinkerton, A. B.; Huang, D.; Cube, R. V.; Hutchinson, J. H.; Struthers, M.; Ayala, J. M.; Vicario, P. P.; Patel, S. R.; Wisniewski, T.; DeMartino, J. A.; Vernier, J.-M. *Bioorg. Med. Chem. Lett.* **2007**, *17*, 807.
27. Butora, G.; Jiao, R.; Parsons, W. H.; Vicario, P. P.; Jin, H.; Ayala, J. M.; Cascieri, M. A.; Yang, L. *Bioorg. Med. Chem. Lett.* **2007**, *17*, 3636.
28. Lagu, B.; Gerchak, C.; Pan, M.; Hou, C.; Singer, M.; Malaviya, R.; Matheis, M.; Olini, G.; Cavender, D.; Wachter, M. *Bioorg. Med. Chem. Lett.* **2007**, *17*, 4382.
29. Carter, P. H.; Brown, G. D.; Friedrich, S. R.; Cherney, R. J.; Tebben, A. J.; Lo, Y. C.; Yang, G.; Jezak, H.; Solomon, K. A.; Scherle, P. A.; Decicco, C. P. *Bioorg. Med. Chem. Lett.* **2007**, *17*, 5455.
30. Xia, M.; Hou, C.; Pollack, S.; Brackley, J.; DeMong, D.; Pan, M.; Singer, M.; Matheis, M.; Olini, G.; Cavender, D.; Wachter, M. *Bioorg. Med. Chem. Lett.* **2007**, *17*, 5964.
31. Yang, L.; Butora, G.; Jiao, R. X.; Pasternak, A.; Zhou, C.; Parsons, W. H.; Mills, S. G.; Vicario, P. P.; Ayala, J. M.; Cascieri, M. A.; MacCoss, M. *J. Med. Chem.* **2007**, *50*, 2609.
32. Xia, M.; Hou, C.; DeMong, D. E.; Pollack, S. R.; Pan, M.; Brackley, J. A.; Jain, N.; Gerchak, C.; Singer, M.; Malaviya, R.; Matheis, M.; Olini, G.; Cavender, D.; Wachter, M. *J. Med. Chem.* **2007**, *50*, 5561.
33. Xue, C.-B.; Wang, A.; Meloni, D.; Zhang, K.; Kong, L.; Feng, H.; Glenn, J.; Huang, T.; Zhang, Y.; Cao, G.; Anand, R.; Zheng, C.; Xia, M.; Han, Q.; Robinson, D. J.; Storace, L.; Shao, L.; Li, M.; Brodmerkel, C. M.; Covington, M.; Scherle, P.; Diamond, S.; Yeleswaram, S.; Vaddi, K.; Newton, R.; Hollis, G.; Friedman, S.; Metcalf, B. *Bioorg. Med. Chem. Lett.* **2010**, *20*, 7473.
34. Xue, C.-B.; Feng, H.; Cao, G.; Huang, T.; Glenn, J.; Anand, R.; Meloni, D.; Zhang, K.; Kong, L.; Wang, A.; Zhang, Y.; Zheng, C.; Xia, M.; Chen, L.; Tanaka, H.; Han, Q.; Robinson, D. J.; Modi, D.; Storace, L.; Shao, L.; Sharief, V.; Li, M.; Galya, L. G.; Covington, M.; Scherle, P.; Diamond, S.; Emm, T.; Yeleswaram, S.; Contel, N.; Vaddi, K.; Newton, R.; Hollis, G.; Friedman, S.; Metcalf, B. A. C. S. *Med. Chem. Lett.* **2011**, *2*, 450.
35. Zhang, X.; Hufnagel, H.; Markotan, T.; Lanter, J.; Cai, C.; Hou, C.; Singer, M.; Opas, E.; McKenney, S.; Crysler, C.; Johnson, D.; Sui, Z. *Bioorg. Med. Chem. Lett.* **2011**, *21*, 5577.
36. Moree, W. J.; Kataoka, K.; Ramirez-Weinhouse, M. M.; Shiota, T.; Imai, M.; Sudo, M.; Tsutsumi, T.; Endo, N.; Muroga, Y.; Hada, T.; Tanaka, H.; Morita, T.; Greene, J.; Barnum, D.; Saunders, J.; Kato, Y.; Myers, P. L.; Tarby, C. M. *Bioorg. Med. Chem. Lett.* **2004**, *14*, 5413.
37. Carter, P. H.; Cherney, R. J.; Batt, D. G.; Brown, G.D.; Duncia, J. V.; Gardner, D. S.; Yang, M. G. *PCT Int. Appl.* WO-2005/020899.
38. MCP-1 receptor binding assay in THP-1 cells:
THP-1 cells were obtained from American Type Culture Collection (Manassas, VA, USA). The THP-1 cells were grown in RPMI-1640 supplemented with 10% fetal bovine serum in a humidified 5% CO_2 atmosphere at 37 °C. The cell density was maintained at 0.5·106 cells/mL. THP-1 cells were incubated with 0.5 nM 125I labeled MCP-1 (Perkin–Elmer Life Sciences Inc., Boston, MA) in the presence of varying concentrations of either unlabeled MCP-1 (R&D Systems, Minneapolis, MN) or test compound for 2 h at 30 °C in a 96 well plates. Cells were then harvested onto a filter plate, dried, and 20 μL of Microscint 20 was added to each well. Plates were counted in a TopCount NXT, Microplate Scintillation & Luminescence Counter (Perkin–Elmer Life Sciences Inc., Boston, MA). Blank values (buffer only) were subtracted from all values and drug treated values were compared to vehicle treated values. 1 μM cold MCP-1 was used for nonspecific binding.
39. MCP-1 induced chemotaxis in THP-1 cells:
MCP-1 induced chemotaxis was run in a 24-well chemotaxis chamber. MCP-1 (0.01 μg/mL) was added to the lower chamber and 100 μL of THP-1 cells (1×10 7 cell/mL) was added to the top chamber. Varying concentrations of test compound were added to the top and bottom chambers. Cells were allowed to chemotax for 3 h at 37 °C and 5% CO_2. An aliquot of the cells which had migrated to the bottom chamber was taken and counted then compared to vehicle.
40. hERG [^{3}H]-astemizole binding experiment: This assay is a 384well in-plate vacuum filtration binding assay. Assay reagents are added into a prepared/blocked 384 well assay plate in the following order: (1) hERG Membrane diluted in assay buffer; (2) test compound; and (3) ^{3}H astemizole diluted in assay buffer. Assay reagents are incubated in the filter plate for 1 h and then washed 6× with ice-cold wash buffer. Plates are allowed to dry overnight at room temperature. The following morning, plates are sealed and scintillant is added to each well. Following a 2-h incubation with scintillant, plates are placed on the TopCount and counted 1 min per well. Data is calculated using raw CPM. Where applicable, IC_{50} values are calculated using raw CPM values. Curves are fitted individually from singlet 11 point dosing curves + 1% DMSO control.
41. Compound **13i**: kinetic solubility at pH 2, 3.5 μM, Caco-2 (Papp, 10^{-6} cm/s), 0.15/2.44, ratio, 16.2; compound **14s**: kinetic solubility at pH 2, 8.9 μM, Caco-2

(Papp, 10^{-6} cm/s): 0.32/3.50, ratio: 10.9; compound **13g**, microsomal stability in rat liver microsome, 25% remain @ 10 min.

42. Patch express experiment: Experiments were performed using HEK293 cells stably expressing the HERG potassium channel. Cells were grown at 37 °C and 5% CO_2 in culture flasks in MEM medium supplemented with 10% heat-inactivated fetal bovine serum, 1% L-glutamine–penicillin–streptomycin-solution, 1% nonessential amino acids (100×), 1% sodium pyruvate (100 mM) and 0.8% geneticin (50 mg/ml). Before use the cells were subcultured in MEM medium in the absence of 5 ml L-glutamine–penicillin–streptomycin. For use in the automated patch-clamp system PatchXpress 7000A (Axon Instruments) cells were harvested to obtain cell suspension of single cells. Extracellular solution contained (mM): 150 NaCl, 4 KCl, 1 $MgCl_2$, 1.8 $CaCl_2$, 10 HEPES, 5 glucose (pH 7.4 with NaOH). Pipette solution contained (mM): 120 KCl, 10 HEPES, 5 EGTA, 4 ATP-Mg_2, 2 $MgCl_2$, 0.5 $CaCl_2$ (pH 7.2 with KOH). Patch-clamp experiments were performed in the voltage-clamp mode and whole-cell currents were recorded with an automated patch-clamp assay utilizing the PatchXpress 7000A system (Axon Instruments). Current signals were amplified and digitized by a Multiclamp amplifier, stored and analyzed by using the PatchXpress, DataXpress software and Igor 5.0 (Wavemetrics). The holding potential was −80 mV. The HERG current (K+-selective outward current) was determined as the maximal tail current at −40 mV after a 2 s depolarization to +60 mV. Pulse cycling rate was 15 s. Before each test pulse a short pulse (0.5 s) from the holding potential to −60 mV was given to determine (linear) leak current. After establishing whole-cell configuration and a stability period, the vehicle was applied for 5 min followed by the test substance by increasing concentrations of 3×10^{-6} M, 10^{-5} M and 3×10^{-5} M. Each concentration of the test substance was applied twice. The effect of each concentration was determined after 5 min as an average current of three sequential voltage pulses. To determine the extent of block the residual current was compared with vehicle pre-treatment. Data are presented as mean values ± standard error of the mean (SEM).
43. Compound **16j**, cryptochrome p450 Inhibition IC50 (μM): 6.8 (3A4), >10 (2C9, 2C19, 2D6, and 1A2).